ELSEVIER

Ceramics International 32 (2006) 61–66

CERAMICS INTERNATIONAL

www.elsevier.com/locate/ceramint

Phase and microstructure evolution in precursor plasma-sprayed YIG coatings

X.Z Guo [a], B.G. Ravi [a,*], Q.Y. Yan [a], R.J. Gambino [a], S. Sampath [a], J. Margolies [a], J.B. Parise [a,b]

[a] *Center for Thermal Spray Research, Department of Materials Science and Engineering, State University of New York, Stony Brook, NY 11794-2275, USA*

[b] *Department of Geosciences and Chemistry Department, State University of New York, Stony Brook, NY 11794-2100, USA*

Received 19 October 2004; received in revised form 12 November 2004; accepted 3 January 2005
Available online 7 March 2005

Abstract

Yttrium iron garnet (YIG) coatings were prepared using a liquid precursor plasma spray (PPS) method. Regular and reverse co-precipitated feedstock sols were directly sprayed through a radio frequency (RF) plasma torch. X-ray diffraction (XRD) analyses revealed the formation of amorphous coating in the as-sprayed condition. Post-annealing treatments resulted into nanostructured garnet coatings and the crystallinity of the coatings increased as a function of increasing annealing temperature. Coating annealed at 1000 °C/h exhibited a saturation magnetization of 65 emu/cc and a coercivity of 37 Oe. PPS approach feeds on molecularly mixed precursor liquids or sols, obviating the need for pre-mixed powders and thus opening up new avenues for developing nanostructured magnetic oxide coatings.

Keywords: A. Films; B. Surface; C. Magnetic properties; Plasma spray

1. Introduction

YIG ($Y_3Fe_5O_{12}$) have attracted much attention in telecommunications and data storage industries due to their interesting magnetic and magneto-optic properties [1]. YIG materials, in ceramics or single crystal form, have been commercially used in microwave circuits for example as resonators, isolators and circulators.

Synthesis of YIG powders via conventional solid-state reaction requires temperatures of ≥1200 °C for several days. To meet the sintering requirements, powders prepared by this method need prolonged grinding which is prone to reduced purity of the material. Several soft chemical approaches have also been reported for synthesis fine YIG powders [2–4]. Nevertheless high sintering temperatures (>1450 °C) and long soaking time (>10 h) are required to make YIG materials with density >97% for device applications.

There are several possible methods, under normal atmospheric conditions, which can be employed for the preparation of magnetic thick films on large ceramic or metal surfaces, such as, spray pyrolysis [5], slurry coating [6] screen-printing [7], and atmospheric plasma spraying [8,9]. The plasma-spray technique has a deposition rate three orders of magnitude larger than the sputtering technique and is a convenient way to produce large overlays on suitable substrates and onto conformal geometries [10]. However for magnetic applications this technique should be developed further in terms of process optimization. Traditional thermal spray process utilizes powder feedstock of premixed composition to develop fine-grained deposits of ceramics. Thermal spray technique coupled with precursor solution chemistry is expected to offer excellent opportunities in making magnetic oxide films in a less expensive way. Precursor plasma spray (PPS) technique utilizes molecularly

* Corresponding author. Tel.: +1 631 632 1168; fax: +1 631 632 7878.
E-mail address: bravi@notes.cc.sunysb.edu (B.G. Ravi).

0272-8842/$30.00
doi:10.1016/j.ceramint.2005.02.001

mixed precursor liquids, and thus avoids the handling/selection of pre-mixed powders was successfully employed to deposit thin/thick films of yttrium garnets [11–13]. The important advantages of PPS include: axial feeding of precursor solution/sol into the larger hot zone which would provide a longer particle residence time, and electrode free nature of RF plasma which avoids the contaminations from the electrodes.

The objective of this study is to develop suitable liquid precursors, identify and correlate the phase, microstructure and magnetic properties of YIG films deposited by PPS. In this paper we report the RF plasma spraying of mixed nitrate sol and the effect of post-heat treatment on phase evolution, microstructure and magnetic properties of YIG coatings.

2. Experimental

2.1. Precursor sol preparation

YIG precursor sol was prepared by chemical co-precipitation method using reagent grade nitrates purchased from Aldrich, Milwaukee, WI, USA. Yttrium nitrate [$Y(NO_3)_3{\cdot}6H_2O$, 99.95% purity], and iron(III) nitrate [$Fe(NO_3)_3{\cdot}9H_2O$, 98+% purity] in 3:5 mol ratio were dissolved in excess of deionized water and mixed thoroughly using a magnetic stirrer. Two types of YIG precipitates namely REGULAR sol (REG-sol) and REVERSE sol (REV-sol) were prepared. In the case REG-sol, the mixed nitrate solution turned into a gelatinous mass with the drop wise addition of ammonia solution (25% ammonium hydroxide, assay 28.0–30.0% NH_3). The gel was washed, filtered out and re-dispersed ultrasonically in de-ionized water. To prepare a REV-sol, the mixed nitrate solution was added drop wise into diluted ammonia solution having a pH of 10. In this case fresh ammonia solution was constantly added to maintain the pH at 10 throughout the precipitation process. Gel so obtained was then washed and ultrasonically dispersed in de-ionized water similar to REG-sol preparation.

2.2. Precursor plasma spraying

Precursor sol's concentration was adjusted to have a final solid content of 30 g/L. For depositing the coatings, the feedstock sol was sprayed on alumina (Al_2O_3) (65 mm × 25 mm × 2 mm) and silicon (Si) (55 mm × 50 mm × 1 mm) substrates using a RF plasma torch (Model PL-100, TEKNA Plasma Systems Inc., Sherbrooke, Canada). The precursor sol was fed into the RF plasma torch and directly gas-atomized into the argon/helium plasma through an atomistic probe. The spray conditions used to form the coatings are presented in Table 1. When the atomized precursor liquid droplets having a size range of 20–70 μm fed through RF Plasma it underwent evaporation followed by pyrolytic decomposition. The average residence time of the particles in the plasma during spraying is around 1 s. In spite of such a short duration, a complete chemical reaction can takes place in micro scale levels within the atomized droplets to form polycrystalline ceramic coating [11,12]. The particles thus formed accelerated towards the substrate where particle bonding and sintering took place to form coatings.

Table 1
RF plasma spray parameters

Parameter	Value
Power (kW)	60
Chamber pressure (kPa)	13–16
Plasma swirl gas (argon) (slpm[a])	25
Plasma sheath gas (argon/helium) (slpm[a])	85/150
Atomized gas	Helium
Feed rate (ml/min)	10–30
Substrate–torch distance (mm)	200 and 250
Traverse speed (cm/s)	2.5
Number of passes (pre-heat/deposit)	4/20

[a] slpm: standard litter per minute.

In the spray experiment, the RF gun was held stationary and the substrate holder was moved horizontally back and forth. The substrate holder was designed to have two base plates so that the substrates were conveniently placed at two different substrate-torch distances (200 and 250 cm) for comparison. Prior to deposition the substrates were pre-heated to a temperature of 400 °C with plasma flame for few seconds. During spraying, the substrate temperature increases steadily from 200 °C to 600 ± 25 °C in about 7 passes and stays at the same temperature until about 25 passes. In a typical spray run, 250 ml of sol was sprayed continuously to produce a coating thickness of ∼70 μm. The reproducibility of the coating with desired composition was ensured by repeating as many as five spray experiments. With an optimum spray condition the coating thickness mainly dependent on the concentration of sol and number of spray passes made.

The phase developed in the coatings was examined by powder X-ray diffraction (SCINTAG/ PAD-V diffractometer) at a scan rate of 2 °/min. using Cu Kα radiation (λ = 1.5408 Å). The decomposition characteristics of dried precursor gel powders were studied by differential thermal analysis (DTA) and thermogravimetry (TG) (NETZSCH, STA 449C). Microstructural analysis was performed by a scanning electron microscope (SEM, LEO/1550). Magnetic measurements were made using a vibrating sample magnetometer (DMS VSM 1660) and the hysteresis loops were recorded at room temperature in fields up to 5 kOe. The saturation magnetization of coatings was obtained after independently measuring the sample volume.

3. Results and discussion

Powder XRD patterns of as-sprayed and post-annealed coatings sprayed using REG-sol are shown in Fig. 1. The XRD pattern indicates the as-sprayed coating predominantly

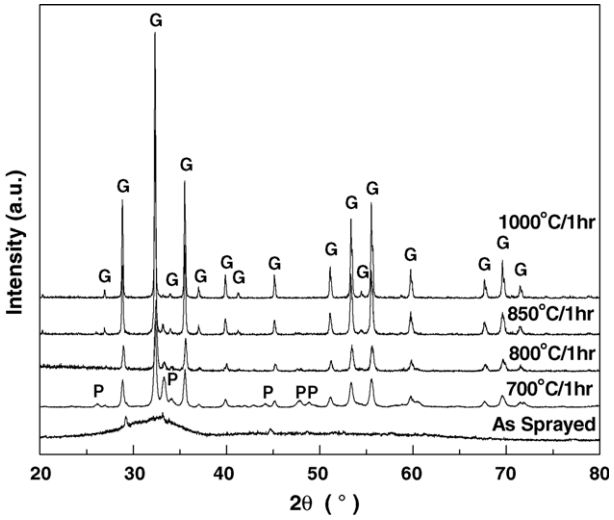

Fig. 1. Powder XRD patterns of as-sprayed and post-annealed coatings. Diffraction lines corresponding to orthorhombic $YFeO_3$ (YIP) phase are denoted as 'P'.

has an amorphous structure. However very small peaks seen in the XRD pattern suggests as-sprayed coating also contain a fraction of amorphous-like crystalline phase. XRD pattern of coating annealed at 700 °C contains Bragg lines corresponding to both garnet and orthorhombic yttrium iron perovskite (YIP) phases. XRD results also revealed that the crystallinity of the coatings increased with increasing annealing temperature. The intensity of peaks corresponding to YIP phase decreased with increase of annealing temperature and diffraction lines in the XRD pattern of coating annealed at 1000 °C/h could be completely indexed to YIG phase. The XRD patterns (not shown) of as-sprayed and annealed coatings made from REV-sol are very similar to that of REG-sol coating shown in Fig. 1.

In the previous work, crystalline yttrium aluminum garnet (YAG) coatings were obtained in the as-sprayed condition when mixed nitrate solution [11] and citrate–nitrate solution [12] sprayed through RF plasma. However in this work, crystalline coating did not achieved in the as sprayed condition. Attempts to increase the plasma temperature resulted into only crystalline YIG powders and not an adhered coating. To gain better insight into the precursor pyrolysis, thermal analysis was performed on the precursor gels dried at 200 °C. A good knowledge of thermal decomposition of the precursors is of prime importance for the optimizing the thermal plasma spray parameters. Combined TG and DTA curves of dried powders of REG- and REV-sol are shown in Figs. 2 and 3, respectively. The first rapid decrease in weight and the exotherms centered in the temperature range 200–550 °C correspond to the decomposition and oxidation of precursors. There was no further weight loss after 600 °C in the case of REG-sol but for REV-sol the weight loss continued until about 780 °C. The exotherm at 715 °C indicates amorphous to crystalline phase transformation of YIG in the case of REG-sol (Fig. 2).

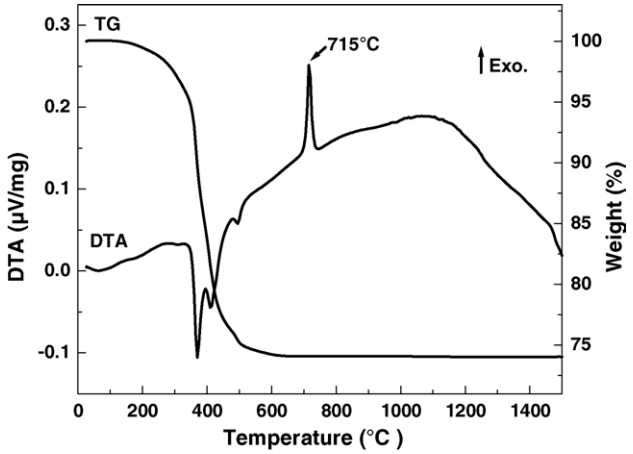

Fig. 2. Combined TG and DTA curves of dried gel obtained by regular co-precipitation (REG-sol).

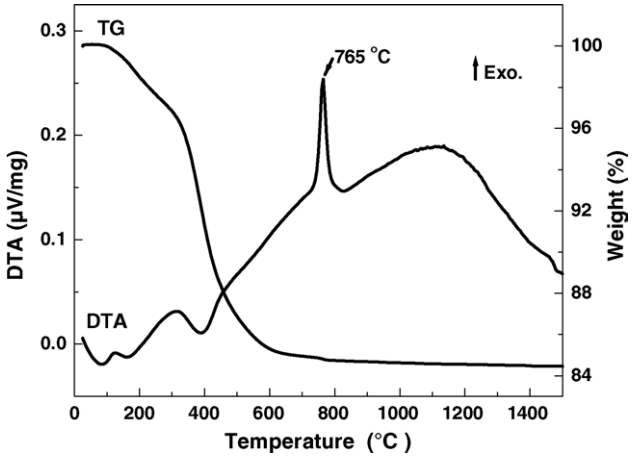

Fig. 3. Combined TGA and DTA curves of dried gel obtained by reverse co-precipitation (REV-sol).

The exothermic peak observed at 763 °C (Fig. 3) indicates the onset of crystallization occurred at a higher temperature in the case of REV-sol. Nevertheless the sharp exotherms observed in the DTA curves of both REG- and REV-sols indicate that the amorphous to crystalline transition occurred over a narrow temperature range and the amorphous phases probably had a similar chemical structure as that of crystalline products. Thermal analysis was also performed on the scrap of the coatings made from REG- and REV-sols and their respective DTA curves are shown in Fig. 4. DTA curves (Fig. 4) indicate both the coatings interestingly exhibited exothermic peaks exactly at 765 °C. This result suggests that irrespective of having different onset of crystallization (Figs. 2 and 3) thermal spraying of both regular and reverse co-precipitated precursors resulted in coatings which have undergone a similar amorphous-crystallization transformation (Fig. 4).

SEM images of surface morphology of REG- and REV-sol sprayed coatings, in the as sprayed condition, are shown in Fig. 5. The microstructure of coating obtained from REV-

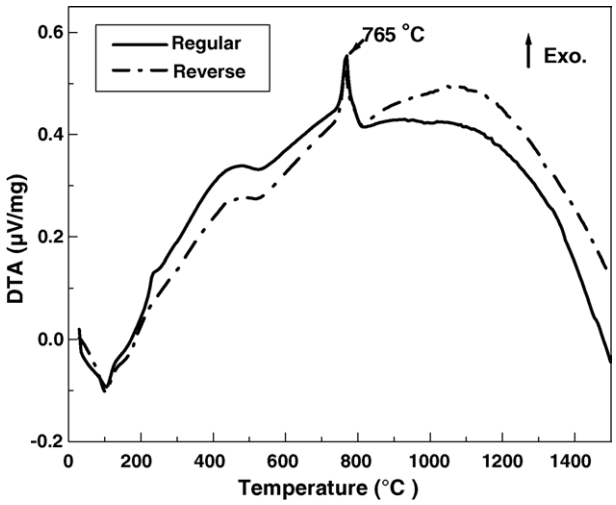

Fig. 4. DTA curves of specks removed from the as-sprayed REG and REV-sol coatings.

sol (Fig. 5b) appears denser when compared to that of coating obtained from REG-sol (Fig. 5a). Surface morphology of as sprayed coating (Fig. 5b) reveals plasma spraying of liquid precursors resulted in deposition of large aggregates having an average size of 65 μm. Fig. 6 shows nanostructured grains in microstructure of the coating annealed at 800 °C, micrograph also revealed post-annealing treatments promoted growth and densification of grains.

To determine the influence of annealing temperature on the crystallite size, calculations of the average crystallite size were performed for the crystallized samples. Scherrer's equation [14], $D = K\lambda/(\beta \cos \theta)$ was used in the calculation, where D is the average crystallite dimension perpendicular to the reflecting phase, λ is the X-ray wavelength, θ is the Bragg angle, and β is the finite-size broadening which is the full width at half-maximum (FWHM) intensity of the main (4 2 0) peak. Instrument line broadening was taken into account while determining β. K is a constant close to unity known as the shape factor of the average crystallite. The average crystallite size, calculated using this equation ranges from 32.3 to 52.7 nm, for coatings annealed at 800 and 1000 °C, respectively. Post-annealing treatments progressively increased the crystallinity of the as sprayed coatings and the amorphous–crystalline transformation gives a nanostructured behavior to the grains of the annealed YIG coatings.

Magnetic properties were measured only for YIG coatings sprayed using REV-sol. The saturation magnetization (M_s) and coercivity (H_c) values measured for as-sprayed and annealed YIG coatings are summarized in Table 2. The room temperature M–H curves of YIG coatings annealed at 800 and 1000 °C are compared in Fig. 7. As-sprayed coating which was predominantly amorphous has a low saturation of 2.5 emu/cc and a high coercivity of 163 Oe. Annealing at 800 °C increased the saturation value to 62.8 emu/cc and decreased the coercivity to 31.2 Oe. The increase in the magnetization of annealed coating can be attributed to the

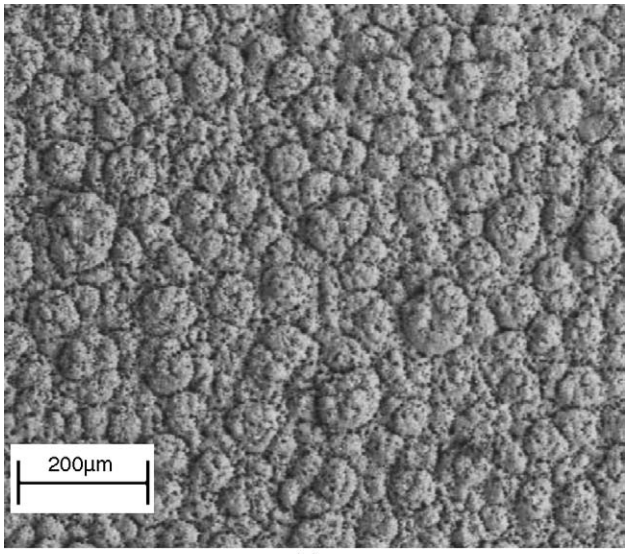

(a)

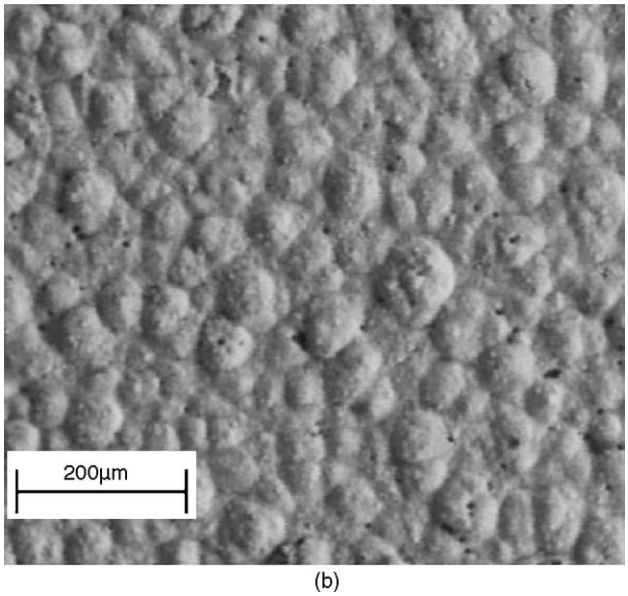

(b)

Fig. 5. SEM micrographs showing the surface features of coatings deposited on alumina substrates using (a) REG-sol and (b) REV-sol.

increased crystallinity and crystallite size with annealing temperature. Coatings annealed at 1000 °C exhibit a saturation magnetization (65.3 emu/cc) and a coercivity (37.4 Oe) values close to that of 800 °C annealed coating. The measured saturation values are low when compared to the bulk saturation magnetization of crystallized YIG which is 26 emu/g [4] or 134.42 emu/cc (based on the theoretical density = 5.17 g/cc). Residual porosities in the coating could significantly reduce the effective volume accounted in the measured magnetization. In order to corroborate this we measured magnetic properties for the sprayed powders where accurate mass of the sample is taken into account. During spraying, large stainless steel base plates (150 mm × 160 mm × 3 mm) were used to hold alumina and Si substrates. Deposits were removed from the base plate, crushed and heat treated at 800 and 1000 °C. XRD

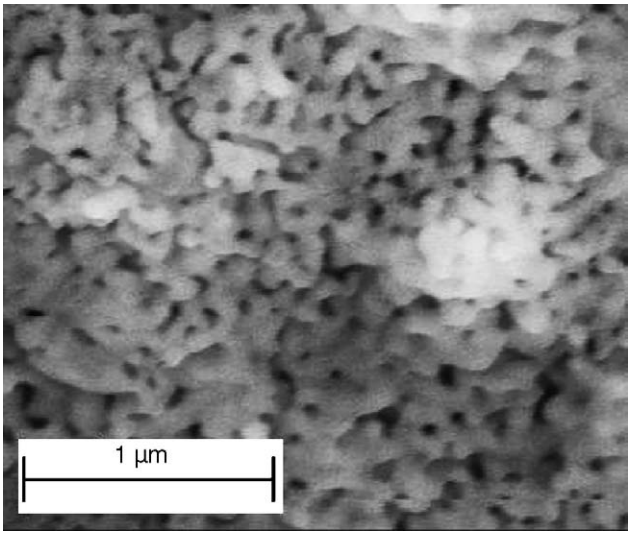

Fig. 6. SEM micrographs showing the grain size and morphology of coating annealed at 800 °C/h.

Table 2
Magnetic properties of YIG coatings and powders

Material (annealing temperature)	M_s (emu/cc)	H_c (Oe)
YIG-coating (as sprayed)	2.54	163
YIG-coating (800 °C)	62.84	31.20
YIG-coating (850 °C)	64.5	32.67
YIG-coating (1000 °C)	65.3	37.42
YIG-powder (800 °C)	14.06[a]	30.60
YIG-powder (1000 °C)	16.68[a]	36.51
YIG-powder (1500 °C)	20.00[a]	1.50

[a] emu/g.

patterns (not shown) indicate annealed powders exhibited phase evolution very similar to that of coatings annealed at same temperatures. Room temperature *M–H* curves of these sprayed powder samples heat treated at 800 and 1000 °C are shown in Fig. 8 and the magnetization values are summarized in Table 2. Powder annealed at 1500 °C for

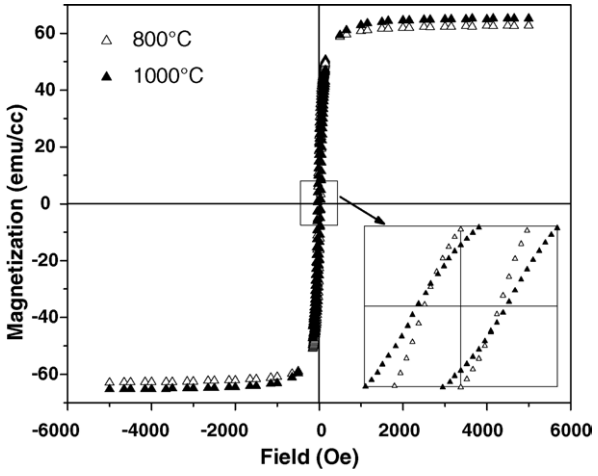

Fig. 7. Room Temperature *M–H* loops of precursor plasma sprayed YIG coatings annealed at 800 and 1000 °C.

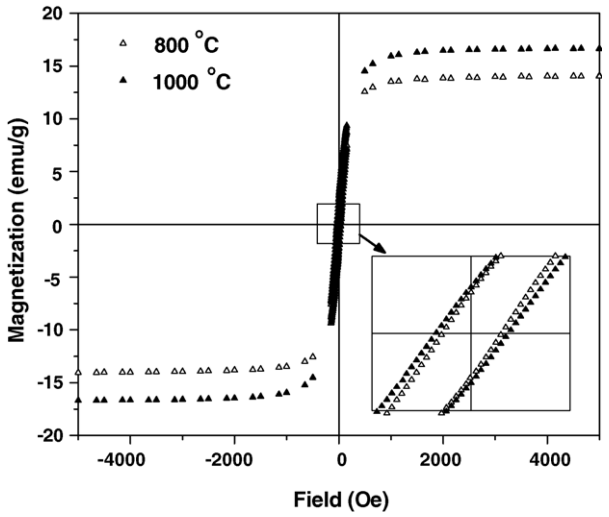

Fig. 8. Room Temperature *M–H* loops of sprayed powders heat-treated at 1000 °C and 1200 °C.

10 h exhibited a saturation magnetization of 20 emu/g and a coercivity of 1.50 Oe. From Table 2, it is also clear that the saturation values of powders annealed at 800 and 1000 °C have only marginally increased compared to that of coating counterparts annealed at the same temperatures. These results indicate that process related defects such as microcracks and voids in the coating were not the main cause for the observed low values of saturation and suggest other factors that influenced the measured properties.

Low saturation magnetization, enhanced coercivity, metastable cation distributions, etc., are some of the phenomena which have been observed in nanoparticles of YIG and various ferrites [2,3,15,16]. A strong reduction in the saturation magnetization of YIG nanoparticales prepared by sol–gel [3] and co-precipitation [17] has also been reported. Pure YIG layers prepared by dip coating of alkoxide sol–gel solution and annealed at 700 °C have exhibited a low value of saturation ~10 emu/g at applied fields of greater than 12,000 Oe [15]. These reports suggested that the nanosized grain features of the crystalline coatings and powders prepared by PPS technique exhibited a similar low magnetization values.

In the YIG formula unit, $Y_3Fe_5O_{12}$, the moments of the Fe^{3+} ions on the octahedral sites are antiferromagnetically coupled to the moments of Fe^{3+} ion on the tetrahedral site. The magnetic moment/formula unit results from Fe^{3+} interaction between a and d site. In general a–d interactions are dominant compared to a–a and d–d interactions [18]. And it is clear that any structural distortion in the Fe^{3+} site may affect the magnetic moment per formula unit. Vaqueiro et al. [2] studied the size dependence of magnetic properties of nanocrystalline YIG prepared by citrate gel process. They further reported structural distortions in the tetrahedral Fe^{3+} sites of nanocrystalline YIG particles using Mössbauer spectrometry results [2]. The low saturation magnetization of YIG nanoparticles was attributed to a non-collinear spin

arrangement at the surface of the particles [2,3]. Non-parallel ionic moments inside each sublattices of ferrimagnetic oxides as a result of negative interactions have been discussed in great detail by Gorter [19]. Based on these reports, we believe that canting or non-parallel arrangement of moments within Fe^{3+} sites could effectively weaken a–d interactions and thus the magnetization of the coating.

4. Conclusions

This paper reports the results obtained in an effort to directly synthesize YIG thick film coatings using a liquid precursor plasma spray method. Amorphous deposit was obtained in the as sprayed condition and a nanostructured coating resulted upon subsequent annealing treatment. The average crystallite size ranges from 32.3 to 52.7 nm for coatings annealed at 800 and 1000 °C, respectively. Microstructural and magnetic property studies revealed better quality coating can be obtained using reverse co-precipitated feedstock sol than regular co-precipitated one. For an optimum spray condition the film thickness is simply dependent on concentration of precursor sol and number of spray passes made on the substrate. This process has the advantage of using inexpensive precursors in a high rate manner, opening up new avenues for developing spherical and nanostructured magnetic oxide coatings.

Acknowledgement

This research was supported by the MRSEC program of the National Science Foundation under award DMR-0080021.

References

[1] Y. Konishi, Microwave Integrated Circuit, Marcel-Dekker, New York, 1991.
[2] P. Vaqueiro, M.A. Lopez-Quintela, J. Rivas, J.M. Greneche, J. Magn. Magn. Mater. 169 (1997) 56.
[3] R.D. Sanchez, J. Rivas, P. Vaqueiro, M.A. Lopez-Quintela, D. Caeiro, J. Magn. Magn. Mater 247 (2002) 92–98.
[4] M. Jafelicci Jr., R.H.M. Godoi, J. Magn. Magn. Mater 226–230 (2001) 1421–1423.
[5] J.L. Deschanvres, M. Langlet, J.C. Joubert, J. Magn. Magn. Mater. 83 (1990) 437–438.
[6] C.S. Kuroda, T. Taniyama, Y. Kitamoto, Y. Yamazaki, J. Magn. Magn. Mater. 241 (2002) 201–206.
[7] C.S. Kuroda, T.Y. Kim, T. Hirano, K. Yoshida, T. Namikawa, Y. Yamazakia, Electrochim. Acta 44 (1999) 3921–3925.
[8] M.T.D. Orlando, A.G. Cunha, J.C.C. Freitas, C.G.P. Orlando, S. Bud'ko, B. Giordanengo, I.M. Sato, L.G. Martinez, E.M. Baggio-Saitovitch, J. Magn. Magn. Mater. 246 (2002) 10–15.
[9] Q. Yan, R.J. Gambino, S. Sampath, L.H. Lewis, L. Li, E. Baumberger, A. Vaidya, H. Xiong, Acta Mater. 52 (2004) 3347–3353.
[10] H. Herman, Sci. Am. 259 (1988) 78.
[11] P.S. Devi, J. Margolis, H.M. Liu, C.P. Grey, S. Sampath, H. Herman, J.B. Parise, J. Am. Ceram. Soc. 84 (2001) 1906.
[12] P.S. Devi, Y. Lee, J. Margolis, J.B. Parise, S. Sampath, H. Herman, J.C. Hanson, J. Mater. Res. 17 (2002) 2846.
[13] X.Z. Guo, B.G. Ravi, P.S. Devi, J.C. Hanson, J. Morgolies, R.J. Gambino, J.B. Parise, S. Sampath, J. Magn. Magn. Mater., in press [doi:10.1016/j.jmmm.2005.01.007].
[14] H.P. Klug, L.E. Alexander, X-Ray Diffraction Procedures for Polycrystalline and Amorphous Materials, second ed., Wiley, New York, 1974, p. 619.
[15] J.-L. Rehspringer, J. Bursik, D. Niznansky, A. Klarikova, J. Magn. Magn. Mater. 211 (2000) 291.
[16] C. Upadhyay, H.C. Verma, S. Anand, J. Appl. Phys. 95 (2004) 5746–5751.
[17] K. Haneda, A.H. Morish, Nucl. Instrum. Methods Phys. Res. B 76 (1993) 132.
[18] R. Pauthenet, Ann. Phys. 3 (1958) 424.
[19] E.W. Gorter, Philips Res. Rep. 9 (1954) 321–365.